# Viscous decay of nonlinear oscillations of a spherical bubble at large Reynolds number

Smith, Warren; Wang, Qian

*DOI:*
10.1063/1.4999940

# Viscous decay of nonlinear oscillations of a spherical bubble at large Reynolds number

W. R. Smith[1, a)] and Q. X. Wang[1]

*School of Mathematics, University of Birmingham, Edgbaston, Birmingham, B15 2TT, UK*

(Dated: 22 July 2017)

The long-time viscous decay of large-amplitude bubble oscillations is considered in an incompressible Newtonian fluid, based on the Rayleigh–Plesset equation. At large Reynolds number, this is a multi-scaled problem with a short time scale associated with inertial oscillation and a long time scale associated with viscous damping. A multi-scaled perturbation method is thus employed to solve the problem. The leading-order analytical solution of the bubble radius history is obtained to the Rayleigh–Plesset equation in a closed form including both viscous and surface tension effects. Some important formulae are derived including: the average energy loss rate of the bubble system during each cycle of oscillation, an explicit formula for the dependence of the oscillation frequency on the energy, and an implicit formula for the amplitude envelope of the bubble radius as a function of the energy. Our theory shows that the energy of the bubble system and the frequency of oscillation do not change on the inertial time scale at leading order, the energy loss rate on the long viscous time scale being inversely proportional to the Reynolds number. These asymptotic predictions remain valid during each cycle of oscillation whether or not compressibility effects are significant. A systematic parametric analysis is carried out using the above formula for the energy of the bubble system, frequency of oscillation and minimum/maximum bubble radii in terms of the Reynolds number, the dimensionless initial pressure of the bubble gases and the Weber number. Our results show that the frequency and the decay rate have substantial variations over the lifetime of a decaying oscillation. The results also reveal that large-amplitude bubble oscillations are very sensitive to small changes in the initial conditions through large changes in the phase shift.

PACS numbers: 47.55.dd

[a)] W.Smith@bham.ac.uk

## I. INTRODUCTION

The nonlinear dynamics of vapour and gas-filled bubbles is of fundamental interest in fluid dynamics, which is associated with the wide and important applications in science and technology[1–4]. Rayleigh initiated the study of bubble dynamics with his investigation of the collapse of an empty spherical bubble in a large mass of liquid[5]. His model, known as the Rayleigh equation, neglected surface tension, liquid viscosity and thermal effects. Plesset developed the full form of the equation and applied it to the problem of travelling cavitation bubbles[6]. The effect of surface tension has been incorporated[7,8] and a viscous term was first included by Poritsky[9], viscous effects being significant for microbubble dynamics and/or long time behaviour of bubbles[2,10]. The resulting equation, known as the Rayleigh–Plesset equation, models the oscillations of a gas-filled spherical bubble in an infinite incompressible liquid. Both the Rayleigh equation and Rayleigh–Plesset equation are nonlinear and therefore numerical methods are often utilised in their solution[10]. However, in recent years, approximate and analytical solutions have been sought to these equations, since analytical analysis is a powerful tool for improved understanding of the qualitative behaviour and trends of phenomena.

Substantial progress has been made in the study of the Rayleigh equation. Accurate explicit analytical approximations for the collapse of an empty spherical bubble have been derived[11]. Each approximation is the product of two factors: a function which models the algebraic singularity at the collapse time; and the sum or partial sum of a power series about the initial time. Furthermore, they showed that their simple analytical expressions are consistent with observations of cavitation data obtained in microgravity. Subsequently, a rigorous justification and explanation for the remarkable accuracy of these approximations to the solutions of the Rayleigh equation has been developed[12]. In the following year, an implicit analytical solution to the Rayleigh equation for an empty bubble (in terms of the hypergeometric function) and for a gas-filled bubble (in terms of the Weierstrass elliptic function) was found[13]. These implicit formulae may be simply solved numerically to obtain the bubble radius. The parametric rational Weierstrass periodic solutions have been found using the connection between the Rayleigh–Plesset equation and Abel's equation[14].

The $N$-dimensional Rayleigh and Rayleigh–Plesset equations were considered by Prosperetti[3] and Klotz[15], where $N \geq 3$. Numerical simulations and analytical results were

employed to investigate the properties of higher dimensional bubbles, new formulae for the Rayleigh collapse time and the frequency of small-amplitude oscillations being obtained. The dynamics were found to be faster in higher dimensions. Subsequently, Kudryashov and Sinelshchikov[16] found implicit analytical solutions to the Rayleigh and Rayleigh–Plesset equations in $N$-dimensions. Van Gorder[17] made a theoretical study for $N$-dimensional bubbles with arbitrary polytropic index of the bubble gas.

Viscous effects are neglected in the above theoretical studies. The purpose of this article is to investigate the long term viscous decay of large-amplitude bubble oscillations in an incompressible Newtonian fluid, to evaluate the time histories of the frequency, amplitude envelope, decay rate and phase shift of bubble oscillation. Microbubble dynamics are associated with important applications such as the cavitation damage to pumps, turbines and propellers[1,4,18–21]. Ultrasound-driven microbubbles are widely used in biomedical technology[22–26], sonochemistry[27] and ultrasonic cavitation cleaning[28].

The viscous bubble dynamics are described by a short time scale associated with inertial oscillation and a long time scale associated with viscous damping, and is thus analysed using a multi-scaled perturbation method. There are two essential challenges in this approach. One of them is to determine the leading-order solution. The other is to remove secular terms (terms in the asymptotic expansion which grow without bound) arising in problems with oscillatory solutions. The equations used to remove the secular terms are known as the secularity conditions. Kuzmak[29] and Luke[30] developed this method for studying nonlinear oscillations and the nonlinear dispersive wave problems. This asymptotic method has successfully determined the decay rate of large-amplitude oscillations of an incompressible viscous drop[31] and a generalization of the Landau equation for travelling waves in two-dimensional plane Poiseuille flow[32]. It is particularly suitable for the multi-scaled nonlinear oscillations which occur in fluid mechanics.

The remainder of the paper is organized as follows. In Sec. II, the Rayleigh–Plesset equation is analysed using a multi-scaled method with a short time scale associated with inertial oscillation and a long time scale with viscous damping. The leading-order problem is solved analytically on the inertial oscillation time scale. At next order, two secularity conditions are obtained to determine the variations of the energy of the bubble system, the oscillation frequency and the minimum and maximum bubble radii, in terms of the long viscous time scale. A further order solution is studied to derive another secularity

condition in order to determine the phase shift on the viscous time scale. In Sec. III, the analytical solutions are firstly compared with experimental observations, numerical solutions of the Rayleigh–Plesset equation and linear theory. A systematic parametric analysis is then carried out with the above theory for the energy of the bubble system, frequency and amplitude of oscillation in terms of the Reynolds number, the dimensionless initial pressure of the bubble gases and the Weber number. Finally, in Sec. IV, this study is summarized and the key outcomes are identified.

## II. ASYMPTOTIC ANALYSIS

### A. Introduction

We study the well-known Rayleigh–Plesset equation for a gas bubble in an incompressible liquid under isothermal conditions[33]

$$\bar{R}\frac{\mathrm{d}^2\bar{R}}{\mathrm{d}\bar{t}^2}+\frac{3}{2}\left(\frac{\mathrm{d}\bar{R}}{\mathrm{d}\bar{t}}\right)^2=\frac{1}{\rho}\left[P_v-P_\infty+\frac{GT}{\bar{R}^3}-\frac{2\sigma}{\bar{R}}\right]-\frac{4\mu}{\rho\bar{R}}\frac{\mathrm{d}\bar{R}}{\mathrm{d}\bar{t}},$$

where $\bar{R}(\bar{t})$ is the spherical bubble radius at time $\bar{t}$, $\rho$ the liquid density, $P_v$ the saturated vapour pressure of the liquid, $P_\infty$ the far-field pressure, $G$ a known constant proportional to both the specific gas constant and the mass of the gas, $T$ the temperature, $\sigma$ the surface tension and $\mu$ the liquid viscosity. The term $GT/\bar{R}^3$ is the partial pressure of bubble gas, assuming that the gas behaves as an ideal gas. For isothermal process considered here, temperature and chemical composition within the bubble are assumed uniform, with water vapour freely entering the bubble with minimal change in surface temperature. Discussions on the heat and mass transfer for oscillating bubbles may reference to Prosperetti[34] and Bergamasco and Fuster[35]. The initial conditions are

$$\bar{R}(0)=\bar{R}_M,\qquad \frac{\mathrm{d}\bar{R}}{\mathrm{d}\bar{t}}(0)=0,$$

in which $\bar{R}_M$ is the initial maximum bubble radius. Here we consider both the viscous and surface tension effects.

We scale this equation using $\bar{R}=\bar{R}_M R$ and $\bar{t}=\bar{R}_M t/U$, where $\Delta=P_\infty-P_v$ and the reference velocity $U=\sqrt{\Delta/\rho}$. The dimensionless Rayleigh–Plesset equation takes the form

$$R\frac{\mathrm{d}^2R}{\mathrm{d}t^2}+\frac{3}{2}\left(\frac{\mathrm{d}R}{\mathrm{d}t}\right)^2=\frac{p_{g0}}{R^3}-\frac{2}{WeR}-1-\frac{4\epsilon}{R}\frac{\mathrm{d}R}{\mathrm{d}t},\tag{1}$$

in which $p_{g0} = GT/\Delta\bar{R}_M^3$ is the dimensionless initial pressure of the bubble gases, $We = \bar{R}_M\Delta/\sigma$ is the Weber number, $Re = \rho U\bar{R}_M/\mu$ is the Reynolds number and $\epsilon = 1/Re$ is a small parameter. The critical parameters in the bubble behaviour are $p_{g0}$ and $We$. The initial conditions are given by

$$R(0) = 1, \qquad \frac{\mathrm{d}R}{\mathrm{d}t}(0) = 0. \tag{2}$$

After multiplying by $R^2\mathrm{d}R/\mathrm{d}t$, equation (1) can be rewritten in the form

$$\frac{\mathrm{d}E}{\mathrm{d}t} = -4\epsilon R\left(\frac{\mathrm{d}R}{\mathrm{d}t}\right)^2, \tag{3}$$

where the energy of a bubble system $E(t)$ is defined as follows

$$E(t) = \frac{R^3}{2}\left(\frac{\mathrm{d}R}{\mathrm{d}t}\right)^2 - p_{g0}\ln(R) + \frac{R^2}{We} + \frac{R^3}{3}. \tag{4}$$

The first term on the right-hand side of (4) is the kinetic energy of the bubble system, the third term is the potential energy associated with surface tension, and the remaining two terms are associated with the potential energy of the compressibility of the bubble gases. This definition of energy, which corresponds to the Hamiltonian function in Feng and Leal[33], remains constant for the inviscid incompressible problem.

The compressible effects of the surrounding liquid are not included in the Rayleigh–Plesset equation, but they are described by the Keller–Miksis equation[33,36,37]. General perturbations of a spherical gas bubble in a compressible and inviscid fluid with surface tension were carried out by Shapiro and Weinstein[38] and Costin, Tanveer, and Weinstein[39]. In particular, they proved that the amplitude of oscillation, in the linearized approximation, decays exponentially, in the form $e^{-\Gamma t}$, $\Gamma > 0$, as time advances. Furthermore the decay rate parameter $\Gamma$ was derived in terms of the Mach number and the Weber number. The damped oscillation of a bubble in a compressible liquid is associated with the loss of energy of a bubble system due to acoustic radiation and/or the emission of shock waves to the far field[40–43].

The Rayleigh–Plesset will predict the energy loss for each cycle due to viscous effects even if acoustic radiation is considered, because the energy loss due to acoustic radiation happens during a very short period at the end of the collapse when viscous effects are insignificant. The damping due to viscous effects is thus mainly contributed during the remaining time when the compressible effects are negligible[43].

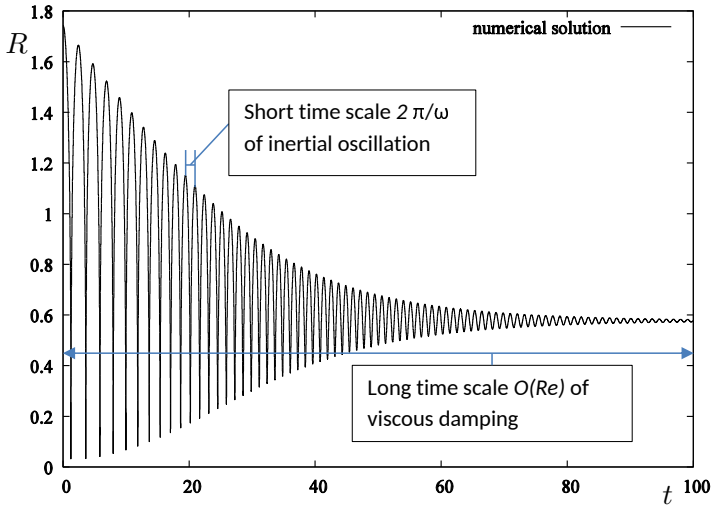


FIG. 1. Typical transient behaviour of a bubble undergoing oscillations in an incompressible viscous fluid, in terms of the bubble radius history $R(t)$. The period $2\pi/\omega$ of inertial oscillation is the short time scale associated with changes in the bubble radius; whereas, the period and minimum/maximum bubble radii vary on a long viscous time scale of the order of the Reynolds number $Re$.

## B. The leading-order solution

A bubble in an incompressible Newtonian fluid undergoes a damped oscillation, with the amplitude and period reducing gradually, as illustrated in Figure 1. The time scale, over which the bubble radius $R$ changes significantly, is the period $2\pi/\omega$ of inertial oscillation, where the (angular) frequency is $\omega$. However, the time scale for the variation of the period (or frequency) and the minimum/maximum bubble radii is the long time scale associated with viscous damping of the order of the Reynolds number $Re$. We therefore introduce two time variables $t_i$ and $t_v$ associated with the inertial and viscous time scales[29,44,45], respectively,

$$\frac{\mathrm{d}t_i}{\mathrm{d}t} = \omega, \tag{5a}$$

$$t_v = \epsilon t, \tag{5b}$$

$$\frac{\mathrm{d}}{\mathrm{d}t} = \omega\frac{\partial}{\partial t_i} + \epsilon\frac{\partial}{\partial t_v}, \tag{5c}$$

where the (angular) frequency of oscillation $\omega$ needs to be chosen so that, in terms of $t_i$, the period of oscillation of the leading-order solution is independent of $t_v$. The period on this $t_i$ scale is then an arbitrary constant which we specify to be $2\pi$ without loss of generality.

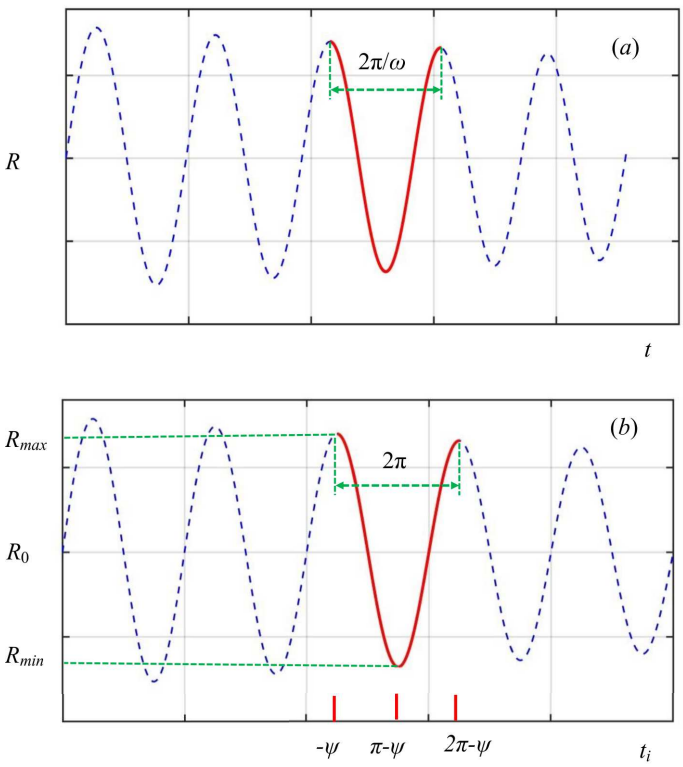


FIG. 2. Schematic of the time history of the radius of an oscillating bubble in terms of $(a)$ the dimensionless time $t$ with oscillation period $2\pi/\omega$ and $(b)$ the inertial oscillation time scale $t_i$ with constant oscillation period chosen to be $2\pi$. The phase shift $\Psi$ is defined by taking $t_i + \Psi = 0$ at $R_0 = R_{max}$ and $t_i + \Psi = \pi$ at $R_0 = R_{min}$.

Figures 2$(a)$ and 2$(b)$ illustrate the time history of an oscillating bubble in terms of the dimensionless time $t$ and the inertial oscillation time $t_i$, respectively.

Using $(5c)$, the Rayleigh–Plesset equation (1) becomes

$$R\left(\omega^2\frac{\partial^2 R}{\partial t_i^2} + 2\epsilon\omega\frac{\partial^2 R}{\partial t_i \partial t_v} + \epsilon\frac{\mathrm{d}\omega}{\mathrm{d}t_v}\frac{\partial R}{\partial t_i} + \epsilon^2\frac{\partial^2 R}{\partial t_v^2}\right) + \frac{3}{2}\left(\omega\frac{\partial R}{\partial t_i} + \epsilon\frac{\partial R}{\partial t_v}\right)^2 = \frac{p_{g0}}{R^3} - \frac{2}{WeR} - 1 - \frac{4\epsilon}{R}\left(\omega\frac{\partial R}{\partial t_i} + \epsilon\frac{\partial R}{\partial t_v}\right). \tag{6}$$

We introduce an expansion for the bubble radius of the form

$$R \sim R_0(t_i, t_v) + \epsilon R_1(t_i, t_v) + \epsilon^2 R_2(t_i, t_v), \tag{7}$$

as $\epsilon \to 0$. At leading order in (6) we obtain

$$\omega^2 R_0\frac{\partial^2 R_0}{\partial t_i^2} + \frac{3}{2}\omega^2\left(\frac{\partial R_0}{\partial t_i}\right)^2 = \frac{p_{g0}}{R_0^3} - \frac{2}{WeR_0} - 1. \tag{8}$$

The higher order equations will be discussed in Sec. II C and Sec. II D. We also introduce an expansion for the energy of the bubble system of the form

$$E \sim E_0(t_v) + \epsilon E_1(t_i, t_v) + \epsilon^2 E_2(t_i, t_v), \tag{9}$$

where the dependence of $E_0$ only on $t_v$ and

$$E_0(t_v) = \omega^2 \frac{R_0^3}{2} \left( \frac{\partial R_0}{\partial t_i} \right)^2 - p_{g0} \ln(R_0) + \frac{R_0^2}{We} + \frac{R_0^3}{3} \tag{10}$$

follow from (3) and (4), respectively.

Equation (8) is readily integrated to yield

$$Q^2 = \omega^2 \left( \frac{\partial R_0}{\partial t_i} \right)^2 = \frac{2}{R_0^3} \left\{ E_0(t_v) + p_{g0} \ln(R_0) - \frac{R_0^2}{We} - \frac{R_0^3}{3} \right\}, \tag{11}$$

where

$$Q = \omega \frac{\partial R_0}{\partial t_i} = \pm \sqrt{\frac{2}{R_0^3} \left\{ E_0(t_v) + p_{g0} \ln(R_0) - \frac{R_0^2}{We} - \frac{R_0^3}{3} \right\}}. \tag{12}$$

The negative sign above is associated with the collapse stage from the maximum bubble radius to the minimum bubble radius and the positive sign above with the expansion stage from the minimum bubble radius to the maximum bubble radius.

For an oscillating bubble, as $\partial R_0/\partial t_i = Q = 0$, $R_0$ reaches its maximum or minimum. Using (11), we define the maximum radius $R_{max}(E_0, p_{g0}, We)$ and the minimum radius $R_{min}(E_0, p_{g0}, We)$ to be the two successive roots of

$$g(R_0, E_0, p_{g0}, We) = 2 \left\{ E_0(t_v) + p_{g0} \ln(R_0) - \frac{R_0^2}{We} - \frac{R_0^3}{3} \right\} = 0 \tag{13}$$

such that $g(R_0, E_0, p_{g0}, We) > 0$ for $0 < R_{min}(E_0, p_{g0}, We) < R_0 < R_{max}(E_0, p_{g0}, We)$. As the bubble oscillates, there are two positive roots of $g(R_0, E_0, p_{g0}, We) = 0$ for given values of $E_0$, $p_{g0}$ and $We$, as illustrated in Figure 3. The parameter regimes associated with bubble oscillation will be discussed in Sec. III.

For an oscillating bubble, the periodicity of $R_0(t_i, t_v)$ in terms of $t_i$ follows from the definition of frequency $\omega = \omega(t_v)$ in $(5a)$, the period having been chosen to be $2\pi$ (see Figure 2$(b)$). Equation (12) shows that $Q$ is an odd function of $t_i$ and therefore $R_0$ is an even function of $t_i$. Accordingly, the dependence of $R_0$ and $Q$ on $t_i$ are fully specified if they are determined on a half period of oscillation. We adopt the half period corresponding to the collapse stage from the maximum bubble radius $R_{max}$ to the subsequent minimum bubble

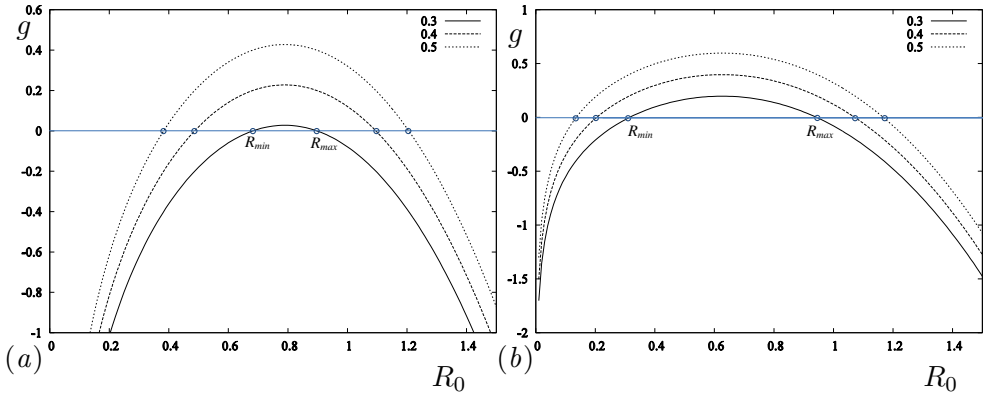


FIG. 3. The nonlinear function $g(R_0, E_0, p_{g0}, We)$ of (13) in terms of $R_0$ for three different values of $E_0 = 0.3$, 0.4 and 0.5 in which the smaller root corresponds to $R_{min}(E_0, p_{g0}, We)$ and the larger to $R_{max}(E_0, p_{g0}, We)$ with parameter values $We = 160$, $(a)$ $p_{g0} = 0.25$ and $(b)$ $p_{g0} = 0.5$.

radius $R_{min}$. Furthermore, if we denote $t_i = -\Psi$ at the maximum bubble radius $R_0 = R_{max}$, then $t_i = \pi - \Psi$ at the minimum bubble radius $R_0 = R_{min}$, where $\Psi(t_v)$ is known as the phase shift (see Figure 2$(b)$). We specify the leading-order solution $Q$ for the collapse stage or $t_i + \Psi(t_v) \in (0, \pi)$ to be

$$Q = \omega \frac{\partial R_0}{\partial t_i} = -\sqrt{\frac{g(R_0, E_0, p_{g0}, We)}{R_0^3}}. \tag{14}$$

The leading-order solution $R_0$ for the collapse stage is then obtained by integrating (14) from $t_i = -\Psi$, at the maximum bubble radius $R_0 = R_{max}$, to $t_i < \pi - \Psi$ as follows

$$\int_{R_{max}(E_0, p_{g0}, We)}^{R_0} \frac{-\sqrt{\hat{R}^3} \mathrm{d}\hat{R}}{\sqrt{g(\hat{R}, E_0, p_{g0}, We)}} = \frac{1}{\omega(E_0(t_v), p_{g0}, We)} \int_{-\Psi(t_v)}^{t_i} \mathrm{d}\hat{t} = \frac{1}{\omega(E_0(t_v), p_{g0}, We)} (t_i + \Psi(t_v)). \tag{15}$$

Otherwise, if $t_i + \Psi(t_v) \notin (0, \pi)$, then $R_0$ and $Q$ may be calculated using the parity and periodicity properties

$$R_0(t_i + \Psi, t_v) = R_0(2\pi - (t_i + \Psi), t_v), Q(t_i + \Psi, t_v) = -Q(2\pi - (t_i + \Psi), t_v), \tag{16a}$$

$$R_0(t_i + \Psi, t_v) = R_0(t_i + \Psi - 2n\pi, t_v), Q(t_i + \Psi, t_v) = Q(t_i + \Psi - 2n\pi, t_v), \tag{16b}$$

for any integer $n$. We thus specify the phase shift $\Psi$ by taking $R_0$ to be even (and $Q$ to be odd) about $t_i + \Psi = n\pi$, with $Q < 0$ for $0 < t_i + \Psi < \pi$. We may then express $\omega$ in terms

of $E_0(t_v)$, $p_{g0}$ and $We$ via

$$\omega(E_0, p_{g0}, We) \int_{R_{min}(E_0,p_{g0},We)}^{R_{max}(E_0,p_{g0},We)} \frac{\sqrt{\hat{R}^3}\mathrm{d}\hat{R}}{\sqrt{g(\hat{R}, E_0, p_{g0}, We)}} = \pi. \tag{17}$$

It remains to determine the energy $E_0(t_v)$ of the bubble system and the phase shift $\Psi(t_v)$. The secularity conditions to derive these quantities will be obtained from the equations for $R_1$ and $R_2$ in Sec. II C and Sec. II D, respectively.

### C. The first correction

At next order in (6) we have

$$\begin{aligned}\omega^2 R_0 \frac{\partial^2 R_1}{\partial t_i^2} + 3\omega^2 \frac{\partial R_0}{\partial t_i}\frac{\partial R_1}{\partial t_i} + \left(\omega^2 \frac{\partial^2 R_0}{\partial t_i^2} + \frac{3p_{g0}}{R_0^4} - \frac{2}{WeR_0^2}\right) R_1 \\ = -2\omega R_0 \frac{\partial^2 R_0}{\partial t_i \partial t_v} - \left(\frac{\mathrm{d}\omega}{\mathrm{d}t_v} R_0 + 3\omega \frac{\partial R_0}{\partial t_v} + \frac{4\omega}{R_0}\right)\frac{\partial R_0}{\partial t_i}.\end{aligned} \tag{18}$$

The right-hand side of (18) contains secular terms which, if not removed, would force $R_1$ to grow and eventually make the asymptotic expansion (7) for $R$ non-uniform. In this subsection, these secular terms are eliminated.

Equation (18) is a linear equation and thus its solution can be constructed from the two linearly independent solutions of its homogeneous equation, using the method of variation of parameters. It can be verified by differentiation of (8) by $t_i$ and $E_0$ that two solutions of the homogeneous problem for (18) are $Q$ and

$$S = \frac{\partial R_0}{\partial E_0}(t_i, t_v; E_0, p_{g0}, We),$$

respectively, in which $\omega(E_0(t_v), p_{g0}, We)$ in (14)-(16) is treated as independent of $E_0$. In order to show that these two solutions are linearly independent, we evaluate the Wronskian $W$ of the two solutions $Q$ and $S$,

$$W = S\frac{\partial Q}{\partial t_i} - Q\frac{\partial S}{\partial t_i},$$

by differentiating (11) with respect to $E_0$ in which, again, $\omega(E_0(t_v), p_{g0}, We)$ is treated as independent of $E_0$. Hence, we obtain

$$W = -\frac{1}{\omega R_0^3} \tag{19}$$

which is apparently nonzero, and thus $Q$ and $S$ are linearly independent.

We apply the method of variation of parameters to solve the inhomogeneous equation for $R_1$ by writing

$$R_1 = \alpha(t_i, t_v)Q + \beta(t_i, t_v)S, \tag{20}$$

where $\alpha(t_i, t_v)$ and $\beta(t_i, t_v)$ are to be determined. As usual in the method of variation of parameters, we impose the following condition

$$Q\frac{\partial \alpha}{\partial t_i} + S\frac{\partial \beta}{\partial t_i} = 0. \tag{21}$$

Substituting (20) into (18) and using (21) yields

$$\omega^2 R_0 \left( \frac{\partial Q}{\partial t_i}\frac{\partial \alpha}{\partial t_i} + \frac{\partial S}{\partial t_i}\frac{\partial \beta}{\partial t_i} \right) = -2\omega R_0 \frac{\partial^2 R_0}{\partial t_i \partial t_v} - \left( \frac{\mathrm{d}\omega}{\mathrm{d}t_v} R_0 + 3\omega \frac{\partial R_0}{\partial t_v} + \frac{4\omega}{R_0} \right) \frac{\partial R_0}{\partial t_i}. \tag{22}$$

We note that $Q$ is periodic, but $S$ is not periodic in $t_i + \Psi$. It is desirable to rewrite equation (20) for $R_1$ in terms of two periodic functions in order to help in identifying the secular terms. The structure of $R_0$ and $Q$ take the form (in view of (14)-(16))

$$R_0 = R_0 \left( \frac{t_i + \Psi(t_v)}{\omega(E_0(t_v), p_{g0}, We)}; E_0(t_v), p_{g0}, We \right), \tag{23a}$$

$$Q = Q \left( \frac{t_i + \Psi(t_v)}{\omega(E_0(t_v), p_{g0}, We)}; E_0(t_v), p_{g0}, We \right). \tag{23b}$$

It follows from differentiation of $R_0$ with respect to $t_v$ that $X$, defined by

$$X = S - \frac{\mathrm{d}\omega/\mathrm{d}t_v(t_i + \Psi)}{\omega^2 \mathrm{d}E_0/\mathrm{d}t_v} Q, \tag{24}$$

is periodic in $t_i + \Psi$, with period $2\pi$, and is even about $t_i + \Psi = n\pi$[46]. The expression for $R_1$ in (20) may now be written in terms of the two periodic functions $Q$ and $X$. Using (24), the solution for $R_1$ given in (20) can be rewritten as

$$R_1 = \gamma Q + \beta X, \tag{25}$$

where

$$\gamma(t_i, t_v) = \alpha(t_i, t_v) + \frac{\mathrm{d}\omega/\mathrm{d}t_v(t_i + \Psi)}{\omega^2 \mathrm{d}E_0/\mathrm{d}t_v} \beta(t_i, t_v).$$

After solving the system of two equations (21) and (22) for the two unknowns $\partial\alpha/\partial t_i$ and $\partial\beta/\partial t_i$, we find

$$\frac{\partial \beta}{\partial t_i} = \frac{R_0^2 Q}{\omega} \left[ -2\omega R_0 \frac{\partial^2 R_0}{\partial t_i \partial t_v} - \left( \frac{\mathrm{d}\omega}{\mathrm{d}t_v} R_0 + 3\omega \frac{\partial R_0}{\partial t_v} + \frac{4\omega}{R_0} \right) \frac{\partial R_0}{\partial t_i} \right], \tag{26}$$

$$\frac{\partial \gamma}{\partial t_i} = \frac{\mathrm{d}\omega/\mathrm{d}t_v}{\omega^2 \mathrm{d}E_0/\mathrm{d}t_v} \beta - \frac{R_0^2 X}{\omega} \left[ -2\omega R_0 \frac{\partial^2 R_0}{\partial t_i \partial t_v} - \left( \frac{\mathrm{d}\omega}{\mathrm{d}t_v} R_0 + 3\omega \frac{\partial R_0}{\partial t_v} + \frac{4\omega}{R_0} \right) \frac{\partial R_0}{\partial t_i} \right]. \tag{27}$$

The suppression of secular terms on the right-hand side of (18) now requires that the right-hand sides of (26) and (27) have zero average over a single cycle of oscillation.

An expression for the first derivative of $E_0$ may be derived by differentiation of (10) as follows

$$\begin{aligned}\frac{\mathrm{d}E_0}{\mathrm{d}t_v} &= \omega\frac{\mathrm{d}\omega}{\mathrm{d}t_v}R_0^3\left(\frac{\partial R_0}{\partial t_i}\right)^2 + \omega^2 R_0^3\frac{\partial R_0}{\partial t_i}\frac{\partial^2 R_0}{\partial t_i \partial t_v} \\ &\quad + R_0^2\frac{\partial R_0}{\partial t_v}\left[\frac{3}{2}\omega^2\left(\frac{\partial R_0}{\partial t_i}\right)^2 - \frac{p_{g0}}{R_0^3} + \frac{2}{WeR_0} + 1\right] \\ &= \omega\frac{\mathrm{d}\omega}{\mathrm{d}t_v}R_0^3\left(\frac{\partial R_0}{\partial t_i}\right)^2 + \omega^2 R_0^3\frac{\partial R_0}{\partial t_i}\frac{\partial^2 R_0}{\partial t_i \partial t_v} - \omega^2 R_0^3\frac{\partial R_0}{\partial t_v}\frac{\partial^2 R_0}{\partial t_i^2}. \end{aligned} \tag{28}$$

Using (28), it is straightforward to show that (26) is equivalent to

$$\frac{\partial \beta}{\partial t_i} = -4\omega R_0\left(\frac{\partial R_0}{\partial t_i}\right)^2 - \frac{1}{\omega}\frac{\mathrm{d}E_0}{\mathrm{d}t_v} - \omega\frac{\partial}{\partial t_i}\left(R_0^3\frac{\partial R_0}{\partial t_i}\frac{\partial R_0}{\partial t_v}\right). \tag{29}$$

As discussed above, the suppression of secular terms in (26) requires

$$\left\langle \frac{\partial \beta}{\partial t_i}\right\rangle = 0,$$

where

$$\langle\ \bullet\ \rangle = \frac{1}{2\pi}\int_{-\Psi}^{2\pi-\Psi} \bullet\ \mathrm{d}t_i$$

denotes the average value over a single cycle of oscillation. The third term on the right-hand side of (29) has zero average due to periodicity, therefore the average of (29) yields

$$\frac{\mathrm{d}E_0}{\mathrm{d}t_v} = -4\left\langle R_0 Q^2\right\rangle. \tag{30}$$

Equation (30) is the first of our secularity conditions and it may be derived much more directly from (3).

We now consider the secularity condition for the phase shift $\Psi(t_v)$. We define a periodic function $\Omega(t_i, t_v)$ in $t_i + \Psi$, with period $2\pi$, which is odd about $t_i + \Psi = n\pi$, by

$$\frac{\partial \Omega}{\partial t_i} = -4\omega^2 R_0\left(\frac{\partial R_0}{\partial t_i}\right)^2 - \frac{\mathrm{d}E_0}{\mathrm{d}t_v}. \tag{31}$$

Integrating

$$\frac{\partial \beta}{\partial t_i} = \frac{1}{\omega}\frac{\partial \Omega}{\partial t_i} - \omega\frac{\partial}{\partial t_i}\left(R_0^3\frac{\partial R_0}{\partial t_i}\frac{\partial R_0}{\partial t_v}\right),$$

we obtain

$$\beta = \beta_0(t_v) + \frac{1}{\omega}\Omega - R_0^3\frac{\partial R_0}{\partial t_v}Q, \tag{32}$$

where $\beta_0(t_v)$ is a further unknown. The structure of the solution (23b) yields

$$\frac{\partial R_0}{\partial t_v} = \frac{1}{\omega}\frac{\mathrm{d}\Psi}{\mathrm{d}t_v}Q + \frac{\mathrm{d}E_0}{\mathrm{d}t_v}X, \tag{33}$$

$$\frac{\partial Q}{\partial t_v} = \frac{1}{Q}\frac{\mathrm{d}E_0}{\mathrm{d}t_v}\left(\frac{1}{R_0^3} + \omega X\frac{\partial Q}{\partial t_i}\right) + \frac{\mathrm{d}\Psi}{\mathrm{d}t_v}\frac{\partial Q}{\partial t_i}, \tag{34}$$

where in each case the last term on the right-hand side is even in $t_i + \Psi$ and the remaining terms are odd in $t_i + \Psi$ about $t_i + \Psi = n\pi$. We also require the result

$$Q\frac{\partial X}{\partial t_i} - X\frac{\partial Q}{\partial t_i} = \frac{1}{\omega R_0^3} - \frac{\mathrm{d}\omega/\mathrm{d}t_v}{\omega^2 \mathrm{d}E_0/\mathrm{d}t_v}Q^2, \tag{35}$$

to rewrite (27) as

$$\frac{\partial \gamma}{\partial t_i} = \frac{\partial}{\partial t_i}\left(R_0^3\frac{\partial R_0}{\partial t_v}X\right) + \frac{4}{\omega}R_0 Q X + \frac{\mathrm{d}\omega/\mathrm{d}t_v}{\omega^2 \mathrm{d}E_0/\mathrm{d}t_v}\left(\beta_0 + \frac{\Omega}{\omega}\right) - \frac{1}{\omega^2}\frac{\mathrm{d}\Psi}{\mathrm{d}t_v}. \tag{36}$$

The first term on the right-hand side of (36) has zero average due to periodicity. The second and fourth terms on the right-hand side of (38) have zero average because they are odd. In order to avoid secularity we require that

$$\frac{\mathrm{d}\Psi}{\mathrm{d}t_v} = \beta_0\frac{\mathrm{d}\omega/\mathrm{d}t_v}{\mathrm{d}E_0/\mathrm{d}t_v}. \tag{37}$$

Unfortunately, this second secularity condition does not complete the analysis of the leading-order solution as $\beta_0(t_v)$ remains undetermined. We define a periodic function $\Lambda(t_i, t_v)$, such that $\langle\Lambda\rangle = 0$, which is even about $t_i + \Psi = n\pi$, by

$$\frac{\partial \Lambda}{\partial t_i} = -4R_0 Q X - \frac{\mathrm{d}\omega/\mathrm{d}t_v}{\omega^2 \mathrm{d}E_0/\mathrm{d}t_v}\Omega.$$

Substituting the equation above into (36) yields

$$\frac{\partial \gamma}{\partial t_i} = \frac{\partial}{\partial t_i}\left(R_0^3\frac{\partial R_0}{\partial t_v}X\right) - \frac{1}{\omega}\frac{\partial \Lambda}{\partial t_i}.$$

Integrating the equation above, we thus have

$$\gamma = \gamma_0(t_v) + R_0^3\frac{\partial R_0}{\partial t_v}X - \frac{1}{\omega}\Lambda. \tag{38}$$

Using our expressions for $\beta$ in (32) and $\gamma$ in (38), the solution for $R_1$ in (25) may now be rewritten as

$$R_1 = \gamma_0(t_v)Q + \beta_0(t_v)X + \frac{1}{\omega}(\Omega X - \Lambda Q), \tag{39}$$

where $\gamma_0$ and $\beta_0$ remain to be determined. However, only the function $\beta_0(t_v)$ is required in the secularity condition (37).

### D. A further secularity condition

In order to complete the analysis of the leading-order solution we require the quantity $\beta_0(t_v)$ in (37). This may be achieved by obtaining a further secularity condition from the equation for $R_2$. Alternatively, as $R_2$ is embedded in $E_2$, a more direct approach to obtaining the required secularity condition is adopted. We substitute the expansions of (7) and (9) for the radius $R(t)$ and the energy $E(t)$, respectively, into (3) and obtain the following equation:

$$\omega\frac{\partial E_2}{\partial t_i}+\frac{\partial E_1}{\partial t_v}=-4R_1Q^2-8R_0Q\left(\omega\frac{\partial R_1}{\partial t_i}+\frac{\partial R_0}{\partial t_v}\right). \tag{40}$$

If we expand (4) and substitute (8), then we have

$$E_1=R_0^3Q\left(\omega\frac{\partial R_1}{\partial t_i}+\frac{\partial R_0}{\partial t_v}\right)-R_0^3R_1\omega^2\frac{\partial^2 R_0}{\partial t_i^2}.$$

Using (19), (20) and (32), the equation above simplifies to become

$$E_1=\beta_0+\frac{1}{\omega}\Omega. \tag{41}$$

The right-hand side of (40) should have zero average over a single cycle of oscillation to avoid secularity. We integrate (40) and (41) to obtain

$$\frac{\mathrm{d}\beta_0}{\mathrm{d}t_v}=-4\left\langle R_1Q^2+2R_0Q\left(\omega\frac{\partial R_1}{\partial t_i}+\frac{\partial R_0}{\partial t_v}\right)\right\rangle. \tag{42}$$

Substituting (33) and (39) into (42) and utilizing parity arguments, we find that

$$\frac{\mathrm{d}\beta_0}{\mathrm{d}t_v}=-4\left\langle \beta_0XQ^2+2R_0Q\left(\omega\beta_0\frac{\partial X}{\partial t_i}+\frac{1}{\omega}Q\frac{\mathrm{d}\Psi}{\mathrm{d}t_v}\right)\right\rangle. \tag{43}$$

Using (35), (37) and (43), a first-order ordinary differential equation for $\beta_0(t_v)$ is obtained

$$\frac{\mathrm{d}\beta_0}{\mathrm{d}t_v}=-4\beta_0\left\langle Q^2X+2R_0\left(\frac{1}{R_0^3}+\omega X\frac{\partial Q}{\partial t_i}\right)\right\rangle. \tag{44}$$

In order to simplify (44) we note that, in view of (30),

$$\frac{\mathrm{d}^2E_0}{\mathrm{d}t_v^2}=-4\frac{\mathrm{d}E_0}{\mathrm{d}t_v}\left\langle Q^2X+2R_0\left(\frac{1}{R_0^3}+\omega X\frac{\partial Q}{\partial t_i}\right)\right\rangle.$$

Therefore,

$$\frac{\mathrm{d}}{\mathrm{d}t_v}\left(\frac{\beta_0}{\mathrm{d}E_0/\mathrm{d}t_v}\right)=0. \tag{45}$$

Integrating (45), we obtain

$$\beta_0=\Psi_1\frac{\mathrm{d}E_0}{\mathrm{d}t_v}, \tag{46}$$

where $\Psi_1$ is a constant. Integrating (37) after the substitution of (46), we determine the phase shift

$$\Psi = \Psi_0 + \omega(E_0(t_v), p_{g0}, We)\Psi_1, \tag{47}$$

where $\Psi_0$ is another constant. We thus obtain a simple formula for the phase shift in terms of the frequency of oscillation. The two constants, $\Psi_0$ and $\Psi_1$, depend on the initial conditions, which will be given in Sec. II E. The leading-order solution is now fully determined up to constants of integration. Alternatively, we note that the viscous term in the Rayleigh–Plesset equation (1) is purely dissipative, so the phase shift satisfies a homogeneous second-order ordinary differential equation. Therefore, it is possible to anticipate the solution (47) in which the $\Psi_0$ term corresponds to the arbitrariness of the origin of $t_i$ in the definition (5$a$) and the $\Psi_1$ term corresponds to the invariance of (1) under translations of $t$ (as discussed in Smith *et al.*[46]).

### E. Initial conditions

It remains to evaluate the initial condition for energy $E_0(0)$ and the constants of integration $\Psi_0$ and $\Psi_1$ (required in (47) to calculate the phase shift $\Psi$) from the initial conditions

$$R(0) \sim 1 + \epsilon a_1, \qquad \frac{\mathrm{d}R}{\mathrm{d}t}(0) \sim 0.$$

We derive the following expansions from these initial conditions

$$R(0)^2 \sim 1 + 2\epsilon a_1, \qquad R(0)^3 \sim 1 + 3\epsilon a_1, \qquad \ln(R(0)) \sim \epsilon a_1.$$

Using (4) and these expansions, we obtain our initial condition for the energy of a bubble system at leading order

$$E_0(0) = \frac{1}{We} + \frac{1}{3},$$

at next order we have

$$E_1(0,0) = a_1\left(\frac{2}{We} + 1 - p_{g0}\right). \tag{48}$$

The initial condition for the phase shift $\Psi(0) = 0$ may then be determined from (15). Using (41), (48) and since $\Omega$ is odd about $t_i + \Psi = 0$, we obtain the result,

$$\beta_0(0) = E_1(0,0) = a_1\left(\frac{2}{We} + 1 - p_{g0}\right). \tag{49}$$

It follows that the constants of integration are given by (46) and (47) in the form

$$\Psi_1 = a_1 \left( \frac{2}{We} + 1 - p_{g0} \right) \Big/ \frac{\mathrm{d}E_0}{\mathrm{d}t_v}(0) \ , \qquad \Psi_0 = -\omega(E_0(0), p_{g0}, We)\Psi_1. \tag{50}$$

A small modification in the initial conditions results in modification of the leading-order solution for bubble radius via the constants of integration for the phase shift.

## III. NUMERICAL RESULTS

As discussed in Feng and Leal[33], in the inviscid limit of (1), dynamics of a gas bubble split into three parameter regimes. In the first regime, the response is typical of an ideal gas bubble when an increase (decrease) in radius is limited by a decrease (increase) in pressure inside the bubble. There is one stable equilibrium and the bubble oscillates for any initial condition $E_0(0)$. In the second parameter regime, the bubble radius may grow without bound or it may oscillate depending on the initial condition $E_0(0)$. In the final parameter regime, when the vapour pressure of the bubble dominates, there are no equilibrium solutions and the bubble radius grows without bound for any initial condition $E_0(0)$. In contrast to an ideal gas bubble, a vapour bubble may fall into any of the three parameter regimes described above, the classification depending on the relative values of surface tension and vapour pressure. The above analysis of the three parameter regimes also holds for viscous bubble dynamics at high Reynolds numbers; however, when the parameters are in an oscillation regime, a bubble undergoes a damped oscillation. Following their results, our numerical results are limited to the first regime in which bubble oscillations occur.

At large Reynolds number, the viscous decay over a single cycle of oscillation is very small. However, over many cycles, these very small amounts of decay accumulate to produce a substantial change in the bubble radius. In this section, we investigate how the Reynolds number $Re$ (or $\epsilon$), the dimensionless initial pressure of the bubble gases $p_{g0}$ and the Weber number $We$ influence bubble oscillations over a long lifetime.

### A. Validation

The average energy loss rate for a bubble system can be rewritten as follows, using (30),

$$\frac{\mathrm{d}E_0}{\mathrm{d}t_v} = \frac{4\omega}{\pi} \int_{R_{min}(E_0,p_{g0},We)}^{R_{max}(E_0,p_{g0},We)} R_0 Q \mathrm{d}R_0.$$

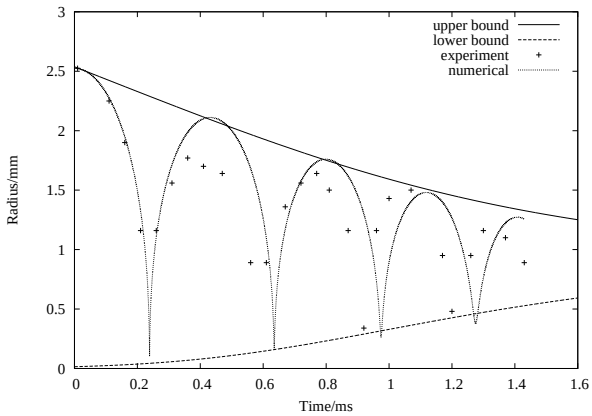


FIG. 4. Comparison of the experiment[10], the numerical solution to (1) and the upper and lower bounds evaluated using the solution to (51) and the roots of (13) for the decaying bubble oscillation in silicone oil. The maximum radius of the bubble is 2.525 mm and the radius at rest is 0.8 mm. The data used for the silicone oil are $\rho = 970$ kgm$^{-3}$, $\sigma = 0.0211$ Nm$^{-1}$ and $\mu = 0.485$ Pas. The dimensionless parameters are $p_{g0} = 0.01$, $We = 1.2 \times 10^4$ and $\epsilon = 0.02$ ($Re = 50$).

Using (14) and (17), the right-hand side may be expressed entirely as a function of $E_0$, $p_{g0}$ and $We$ as follows

$$\frac{\mathrm{d}E_0}{\mathrm{d}t_v} = -4 \frac{\displaystyle\int_{R_{min}(E_0,p_{g0},We)}^{R_{max}(E_0,p_{g0},We)} \sqrt{\frac{2}{\hat{R}}\left\{E_0 + p_{g0}\ln(\hat{R}) - \frac{\hat{R}^2}{We} - \frac{\hat{R}^3}{3}\right\}}\mathrm{d}\hat{R}}{\displaystyle\int_{R_{min}(E_0,p_{g0},We)}^{R_{max}(E_0,p_{g0},We)} \frac{\sqrt{\hat{R}^3}\mathrm{d}\hat{R}}{\sqrt{2\left\{E_0 + p_{g0}\ln(\hat{R}) - \frac{\hat{R}^2}{We} - \frac{\hat{R}^3}{3}\right\}}}}. \tag{51}$$

Equation (51) allows the calculation of the energy $E_0(t_v)$ without prior knowledge of the leading-order solution $R_0$. From this equation we deduce that $\mathrm{d}E_0/\mathrm{d}t_v = f(E_0, p_{g0}, We)$, where $f(E_0, p_{g0}, We)$ is the right-hand side of (51), and thus $\mathrm{d}E_0/\mathrm{d}t = f(E_0, p_{g0}, We)/Re$. Therefore the average loss rate of the energy is inversely proportional to the Reynolds number $Re$.

In the following comparisons of asymptotic and numerical solutions, the NAG routine D02EJF is used for solving the Rayleigh–Plesset equation (1), Euler's method for the first derivative in (51), the NAG routine D01ATF for the integrals in (51) and the bisection algorithm for the roots of (13).

There are circumstances under which a bubble undergoes free oscillations for many cycles without significant acoustic radiation and/or the emission of shock waves. A bubble may

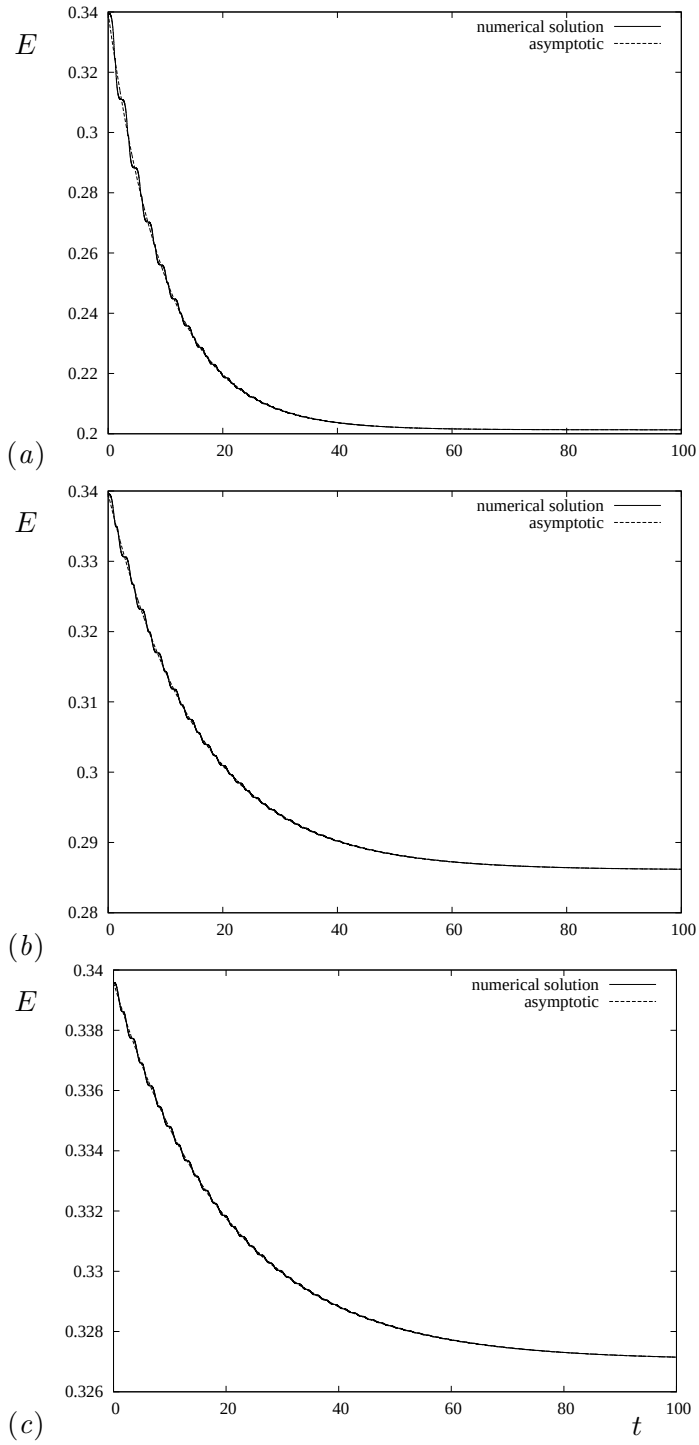


FIG. 5. Comparison of the numerical solution to (1) and the solution of the first-order ordinary differential equation for the energy (51). The parameter values are $p_{g0} = 0.25$ for $(a)$, $p_{g0} = 0.5$ for $(b)$, $p_{g0} = 0.75$ for $(c)$, $We = 160$ and $\epsilon = 10^{-2}$ $(Re = 100)$.

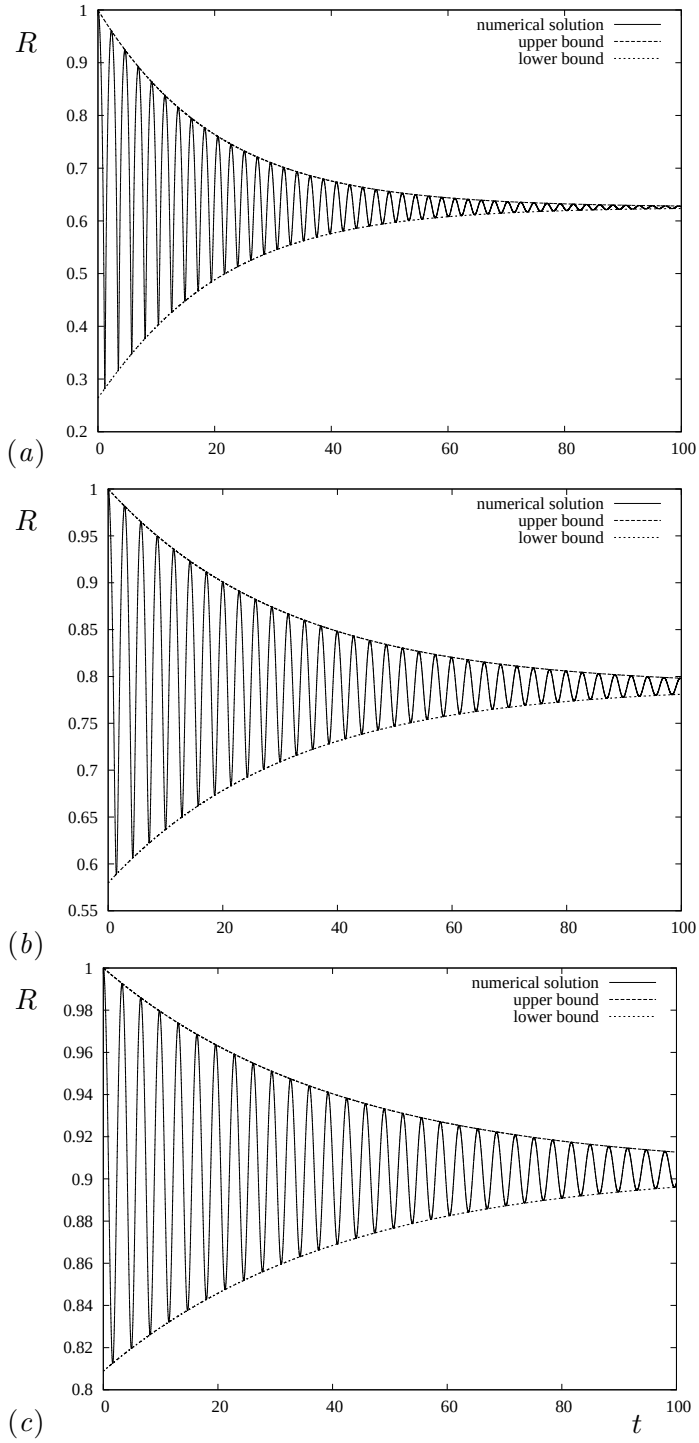


FIG. 6. Comparison of the numerical solution to (1) and the upper and lower bounds evaluated using the solution to (51) and the roots of (13). The parameter values are $p_{g0} = 0.25$ for $(a)$, $p_{g0} = 0.5$ for $(b)$, $p_{g0} = 0.75$ for $(c)$, $We = 160$ and $\epsilon = 10^{-2}$ ($Re = 100$).

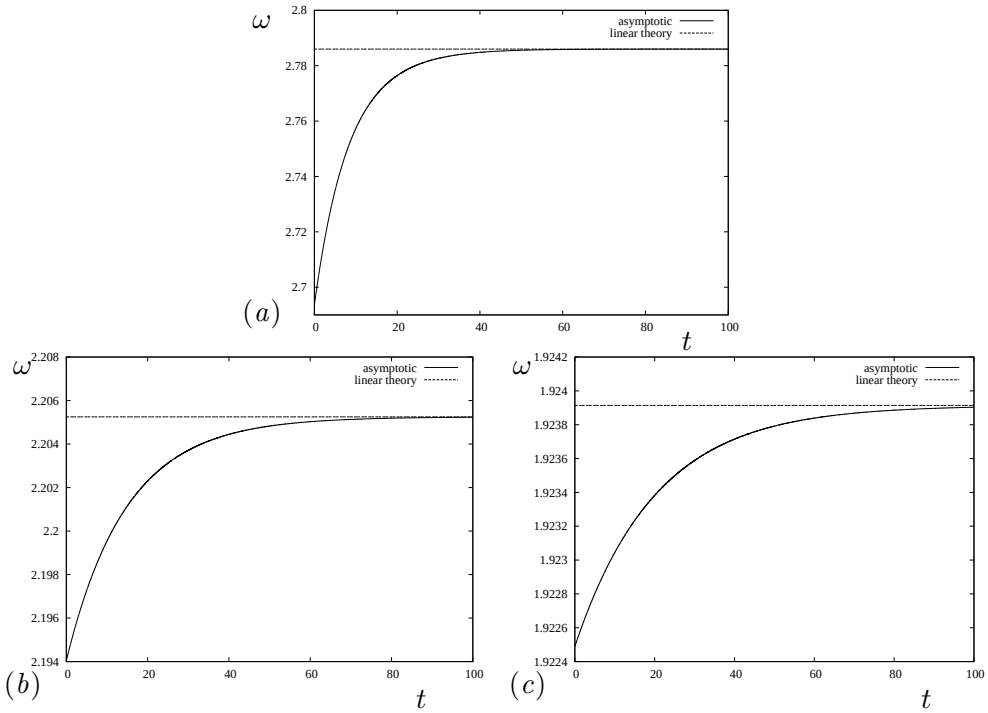


FIG. 7. Comparison of the frequency obtained using (17) and linear theory (52). The parameter values are $p_{g0} = 0.25$ for $(a)$, $p_{g0} = 0.5$ for $(b)$, $p_{g0} = 0.75$ for $(c)$, $We = 160$ and $\epsilon = 10^{-2}$ $(Re = 100)$.

oscillate in a spherical shape for many cycles in a liquid with high viscosity and/or high surface tension[10,47]. The compressible effects are the order of the Mach number $M = U/c$, where $c$ is the speed of sound in the liquid and the viscous effects are the order of $1/Re$. In the case of high viscosity, we may thus quantify the conditions under which viscosity is the dominant decay mechanism by the restriction

$$M \ll \frac{1}{Re} \ll 1 \qquad \text{or} \qquad \frac{U}{c} \ll \frac{\mu}{\rho U \bar{R}_M} \ll 1.$$

In the experiments of Lauterborn and Kurz[10] (figure 32), the compressible effects are negligible due to high surface tension. The agreement of the experiment and our asymptotic analysis is shown in Figure 4.

We now perform three integrations of (51) with the Weber number $We = 160$ and three different values of the minimum pressure at the maximum radius during the first cycle of oscillation $p_{g0}$: $p_{g0} = 0.25$, $p_{g0} = 0.5$ and $p_{g0} = 0.75$. In each case, a full numerical solution of the Rayleigh–Plesset equation (1) is also obtained from a corresponding initial condition

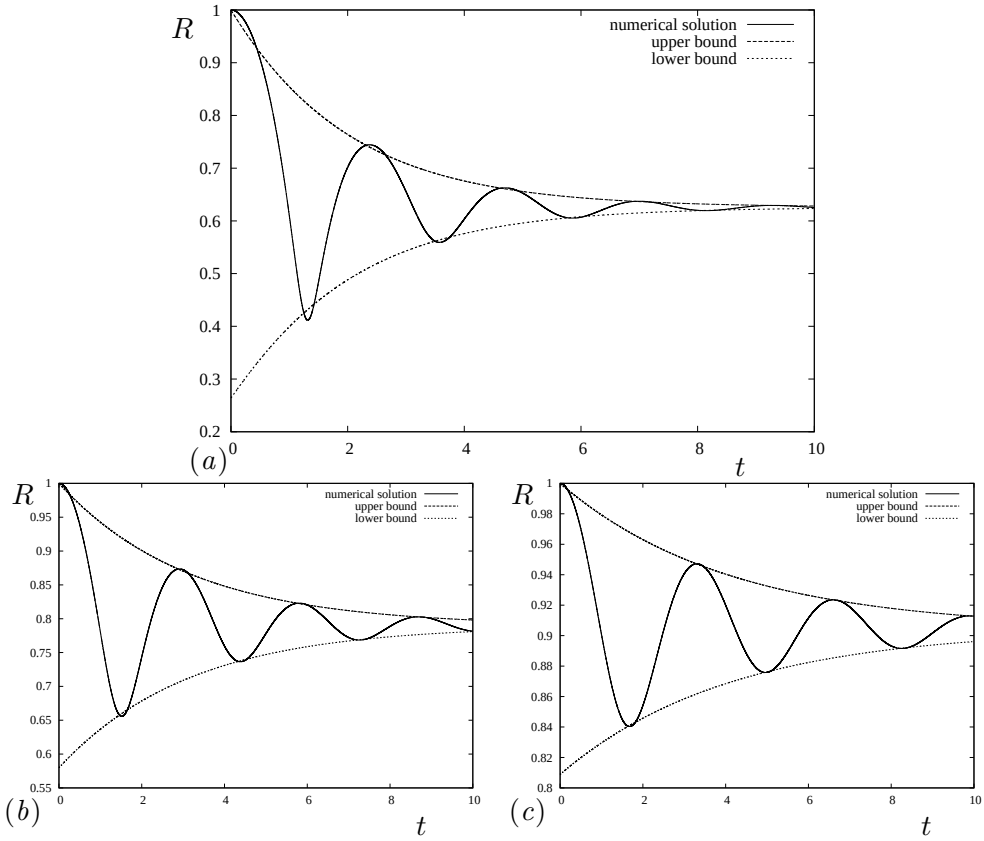


FIG. 8. Comparison of the numerical solution to (1) and the upper and lower bounds evaluated using the solution to (51) and the roots of (13). The parameter values are $p_{g0} = 0.25$ for $(a)$, $p_{g0} = 0.5$ for $(b)$, $p_{g0} = 0.75$ for $(c)$, $We = 160$ and $\epsilon = 10^{-1}$ $(Re = 10)$.

using the maximum bubble radius. Figure 5 compares the solution of (51) with the numerical solution of the Rayleigh–Plesset equation (1) for the time history of the energy of the bubble system for these three values of $p_{g0}$, $We = 160$ and $\epsilon = 10^{-2}$ $(Re = 100)$, the agreement being excellent in all three cases for the entire lifetime of the damped oscillations. The energy of the bubble system decreases with time and its rate of change reduces with time too, reaching a constant during the later stages. There are slight discrepancies between the analytical and numerical results within each cycle of oscillation. This is because the average energy loss rate during each cycle of oscillation is calculated in the analytic approach using (51), which does not track the energy history within each cycle of oscillation. The figures show clearly that the analytical and numerical results of the time history of the energy agree well at the end of each cycle of oscillation.

The amplitude envelope of the oscillations are easily determined from $E_0(t_v)$ using the

roots of (13). Figure 6 compares the upper and lower bounds of the time history of the bubble radius, $R_{max}$ and $R_{min}$, with a full numerical solution of (1), the agreement again being excellent for hundreds of cycles of oscillation. The maximum radius decreases with time, the minimum radius increases with time, and their rates of change first increase and then decrease with time, both reaching the same constant equilibrium bubble radius during the later stages. Comparing the results for $p_{g0} = 0.25$, 0.5 and 0.75, one can see that the damping is enhanced as $p_{g0}$ decreases, the bubble reaches the equilibrium faster at a smaller value of the dimensionless initial pressure of the bubble gases.

The corresponding frequencies, which are evaluated using equation (17), are compared with linear theory in Figure 7. Plesset and Prosperetti[48] provide a review of the linear theory. In the linear theory, frequency is given by

$$\frac{1}{R_{eq}}\sqrt{\frac{3p_{g0}}{R_{eq}^3} - \frac{2}{WeR_{eq}}}. \tag{52}$$

The frequency of the present nonlinear theory shows significant variation over the lifetime of the oscillations. The frequency increases rapidly during the early stages and its rate of change decreases with time, reaching a constant during the later stages. Our perturbation method and the linear theory agree when the deviation from the equilibrium radius is small; that is $R_{max} - R_{min} \ll 1$.

Figure 8 provides a further comparison between the upper and lower bounds, $R_{max}$ and $R_{min}$, with a full numerical solution of (1) at $\epsilon = 0.1$ ($Re = 10$). The upper and lower bounds in Figure 8 are only modified by a scaling in time from Figure 6, which is given by (5$b$). The errors in our asymptotic approach are of the order of $\epsilon$ or $1/Re$[45]. As expected for the lower Reynolds number, the agreement is not as accurate as in Figure 6, but it is still very good. Comparing the results for $Re = 100$ in Figure 6 and $Re = 10$ in Figure 8, one can see that the damping is enhanced significantly as $Re$ decreases.

## B. The behaviour in each cycle

Within each cycle the bubble oscillation depends on three state variables, the dimensionless initial pressure of the bubble gases $p_{g0}$, the Weber number $We$ and the dimensionless energy $E_0$ of the bubble system, the last is a constant during each cycle of oscillation to a first order approximation. We thus analyze the dependence of the frequency of oscillation,

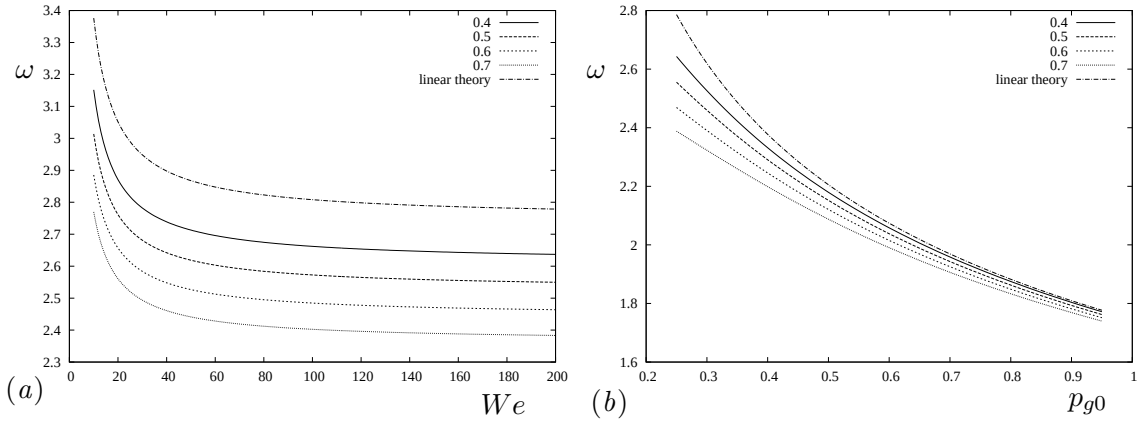


FIG. 9. The frequency of oscillation (17) as a function of $(a)$ the Weber number $We$ with $p_{g0} = 0.25$ and $(b)$ the parameter $p_{g0}$ with $We = 160$ for four values of energy $E_0 = 0.4, 0.5, 0.6, 0.7$. The linear theory (52) is shown for comparison.

minimum and maximum bubble radii in terms of $p_{g0}$, $We$ and $E_0$. Figure 9 shows the dependence of the frequency of oscillation $\omega$ on the energy $E_0$ (or equivalently amplitude), the parameters $p_{g0}$ and $We$. The frequency of oscillation decreases with the energy $E_0$, $p_{g0}$ and $We$. In both the linear and nonlinear theories, the frequency has large variations for a change in the quantities. The linear theory will significantly overestimate the frequency for bubbles oscillating with large energies and amplitudes.

Figure 10 shows the dependence of the minimum bubble radius $R_{min}$ on the energy $E_0$ and the parameters $p_{g0}$ and $We$. The minimum radius decreases rapidly with $E_0$ and increases rapidly with $p_{g0}$, but it is, to a large extent, independent of the parameter $We$.

The dependence of the maximum bubble radius $R_{max}$ on the energy $E_0$ and the parameters $p_{g0}$ and $We$ is shown in Figure 11. The maximum bubble radius increases with $E_0$, $p_{g0}$ and $We$.

## C. The behaviour over many cycles

Figure 12 shows the effect of a variation of the parameter $p_{g0}$ on the long-time history of the energy, the maximum bubble radius and the frequency. The simulations all start from the same initial radius and energy. The energy increases, the maximum bubble radius increases and the frequency decreases for larger $p_{g0}$.

The conventional approach to viscous decay in fluid mechanics is to introduce a decay

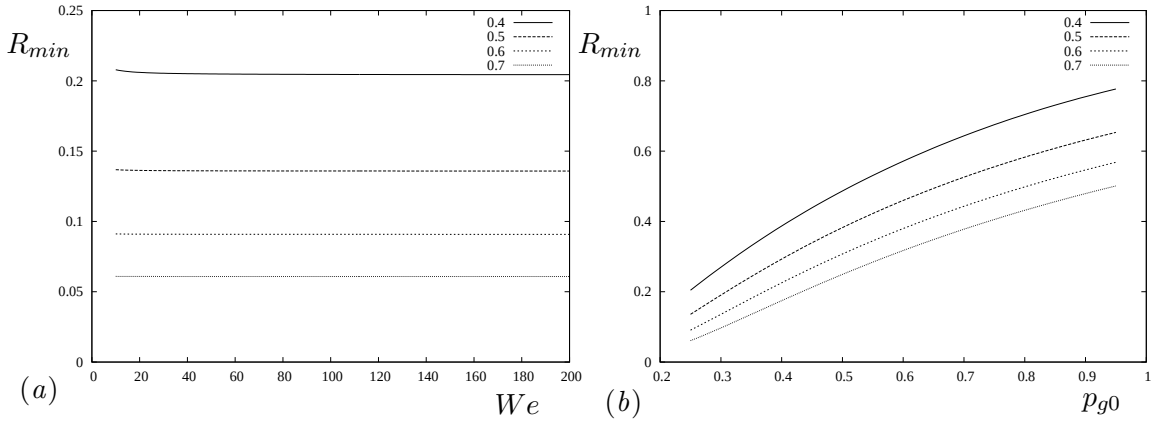


FIG. 10. The minimum bubble radius $R_{min}$ as a function of $(a)$ the Weber number $We$ with $p_{g0} = 0.25$ and $(b)$ the parameter $p_{g0}$ with $We = 160$ for four values of energy $E_0 = 0.4$, 0.5, 0.6, 0.7.

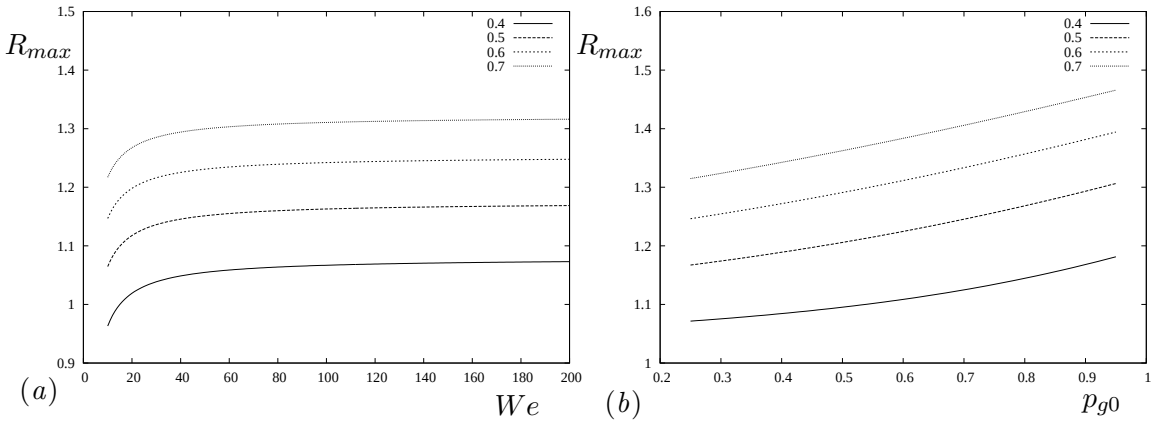


FIG. 11. The maximum bubble radius $R_{max}$ as a function of $(a)$ the Weber number $We$ with $p_{g0} = 0.25$ and $(b)$ the parameter $p_{g0}$ with $We = 160$ for four values of energy $E_0 = 0.4$, 0.5, 0.6, 0.7.

rate (see, for example, Lamb[49]). In order to adopt this approach for spherical bubbles, the maximum bubble radius may be approximated by the expression

$$R_{max}(E_0, p_{g0}, We) = R_{eq}(p_{g0}, We) + \alpha(E_0, p_{g0}, We)\exp(-\lambda(E_0, p_{g0}, We)t_v), \tag{53}$$

where $\alpha(E_0, p_{g0}, We)$ is the amplitude, $\lambda(E_0, p_{g0}, We)$ represents the decay rate and $R_{eq}(p_{g0}, We)$ is the appropriate solution of the cubic equation

$$R^3 + \frac{2}{We}R^2 - p_{g0} = 0. \tag{54}$$

Equation (54) is obtained by setting the time derivatives to zero in (1). If we adopt this definition, then the variation of decay rate is shown in Figure 13. As large values of $p_{g0}$

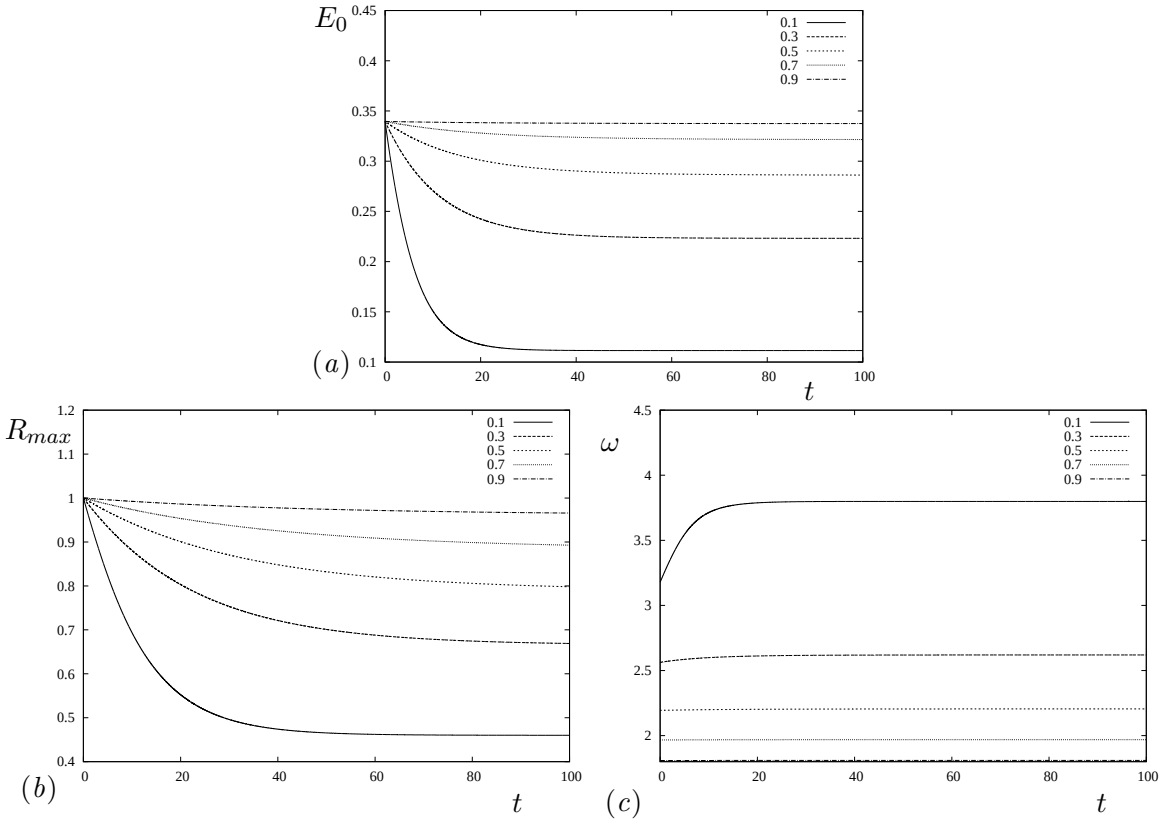


FIG. 12. The time history of the energy of the bubble system $E_0$ in $(a)$, the maximum bubble radius $R_{max}$ in $(b)$ and the frequency $\omega$ in $(c)$ for five values of the parameter $p_{g0} = 0.1$, 0.3, 0.5, 0.7, 0.9, $We = 160$ and $\epsilon = 10^{-2}$ $(Re = 100)$.

limit the range of energies (see Figure 5$(c)$), only one energy is plotted in Figure 13$(b)$. The decay rate increases with decreasing energy $E_0$ and with decreasing parameters $p_{g0}$ and $We$, it being clear that linear theory will significantly overestimate the decay rate for large-amplitude spherical bubble oscillations. We note that the variation of $R_{max}$ does not follow equation (53) for the smallest values of $E_0$, it having been previously reported that small-amplitude bubble oscillations decay algebraically for long times[50].

### D. Sensitivity of the solution to small changes in the initial conditions

We now illustrate how an order $\epsilon$ modification in the initial conditions may produce an order one change in the solution via the phase shift $\Psi$. We adopt $We = 160$, $p_{g0} = 0.1$, $\epsilon = 10^{-2}$ and different values of $a_1$ in Sec. II E. Numerical solutions of the Rayleigh–Plesset

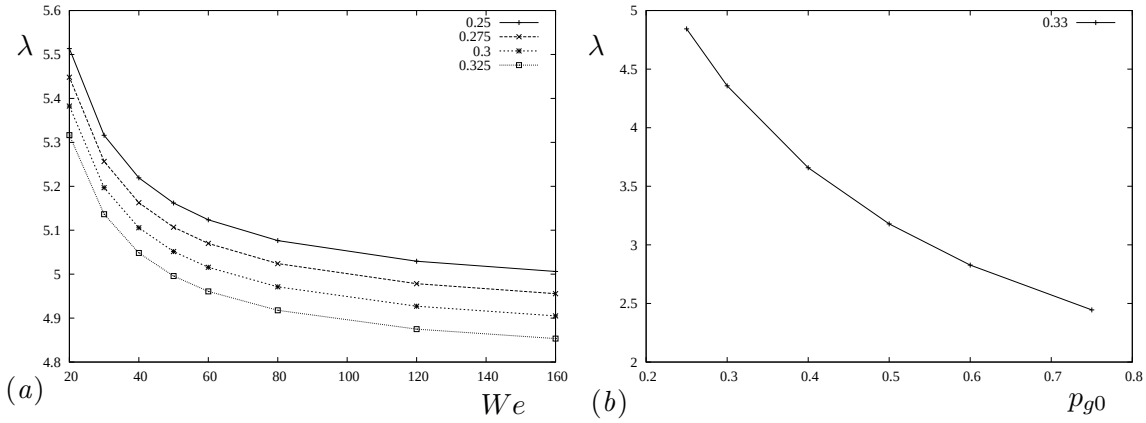


FIG. 13. The decay rate $\lambda$ as a function of $(a)$ Weber number $We$ for $p_{g0} = 0.25$ and four values of $E_0 = 0.25$, 0.275, 0.3, 0.325 and $(b)$ the parameter $p_{g0}$ for $We = 160$ and $E_0 = 0.33$. The decay rate $\lambda$ is defined in equation (53).

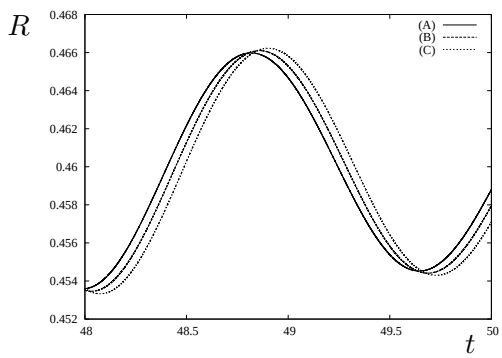


FIG. 14. Comparison of the numerical solution of the Rayleigh–Plesset equation (1) with $We = 160$, $p_{g0} = 0.1$, $\epsilon = 10^{-2}$ ($Re = 100$) and three initial conditions: (A) $R(0) = 1 - \epsilon$ and $\dot{R}(0) = 0$, (B) $R(0) = 1$ and $\dot{R}(0) = 0$, and (C) $R(0) = 1 + \epsilon$ and $\dot{R}(0) = 0$. These results illustrate the linear dependence on $a_1$ in (50).

equation (1) which exhibit the linear dependence on $a_1$ in (50) are shown in Figure 14 with $a_1 = -1$, 0 and 1. Large-amplitude bubble oscillations are extremely sensitive to small changes in their initial conditions.

## IV. SUMMARY AND CONCLUSIONS

A theoretical study has been carried out to investigate the viscous decay of large-amplitude oscillations of a spherical bubble in an incompressible Newtonian fluid. At large

Reynolds number, this is a multi-scaled problem with a short time scale associated with inertial oscillation and a long time scale associated with viscous damping, the ratio of viscous and inertial oscillation time scales being the Reynolds number. A multi-scaled perturbation method is thus employed to solve the Rayleigh–Plesset equation. The leading-order analytical solution of the bubble radius history is obtained to the Rayleigh–Plesset equation in a closed form including both viscous and surface tension effects.

The techniques of strongly nonlinear analysis result in several important analytical formulae including: (i) an explicit expression for the average energy loss rate for the bubble system for each cycle of oscillation, which allows the calculation of the energy without prior knowledge of the bubble radius history, (ii) an explicit formula for the dependence of the frequency of oscillation on the energy, and (iii) implicit formulae for the maximum and minimum radii of the bubble during each cycle of oscillation. Our theory shows that the energy of the bubble system and the frequency of oscillation do not change during the time scale of inertial oscillation to a first order of approximation, the energy loss rate on the long viscous time scale being inversely proportional to the Reynolds number.

These asymptotic predictions have excellent agreement with the numerical solutions of the Rayleigh–Plesset equation over the lifetime of the damped oscillations of a transient bubble (for hundreds of cycles of oscillation) and correlate with the linear theory. Systematic parametric analyses are carried out with the above formulae for the energy of the bubble system, frequency of oscillation and minimum/maximum bubble radii in terms of the Reynolds number, the dimensionless initial pressure of the bubble gases and the Weber number. A series of phenomena are observed, which may be summarized as follows.

Over the long lifetime of a decaying oscillation, the energy of a bubble system, amplitude and frequency of oscillation have large variations. The energy of the bubble system decreases with time and its rate of change reduces with time too, reaching a constant ultimately. The maximum radius decreases with time, the minimum radius increases with time, and their rates of change first increase and then decrease with time, both reaching the same constant ultimately. The frequency increases rapidly during the early stages and its rate of change decreases with time, reaching a constant during the later stages.

The frequency, maximum/minimum bubble radii and their changing rates have been shown to have strong dependence on the energy of a bubble system $E_0$, $p_{g0}$ and $We$. The frequency of oscillation decreases with $E_0$, $p_{g0}$ and $We$. The minimum radius decreases

rapidly with $E_0$ and increases rapidly with $p_{g0}$, but it is, to a large extent, independent of the parameter $We$. The maximum bubble radius increases with $E_0$, $p_{g0}$ and $We$.

Our results also show that linear theory will significantly overestimate the frequency and decay rate of spherical bubble oscillation. The phase shift for decaying bubble oscillations has two constants of integration, these two constants having been shown to depend on small perturbations in the initial conditions. In this sense, large-amplitude bubble oscillations are very sensitive to changes in the initial conditions with the phase being shifted either backwards or forwards. Furthermore, large-amplitude non-spherical bubble oscillations will also exhibit similar sensitivity as it is a consequence of the nonlinearity at leading order. Linear and weakly nonlinear analysis will not predict such sensitivity.

## A. Summary of analytical results

In this final subsection, the three main analytical results are summarized for the convenience of readers. The results are provided in the dimensionless form. The reference length and pressure are chosen as the maximum bubble radius $\bar{R}_M$ during the first cycle of oscillation and $\Delta = P_\infty - P_v$, respectively, where $P_\infty$ is the ambient pressure and $P_v$ is the saturated vapour pressure.

Firstly, the average loss rate of the energy $E_0$ of a bubble system may be written as follows

$$\frac{\mathrm{d}E_0}{\mathrm{d}t} = -\frac{4}{Re}\frac{\displaystyle\int_{R_{min}(E_0,p_{g0},We)}^{R_{max}(E_0,p_{g0},We)} \sqrt{\frac{2}{\hat{R}}\left\{E_0 + p_{g0}\ln(\hat{R}) - \frac{\hat{R}^2}{We} - \frac{\hat{R}^3}{3}\right\}}\mathrm{d}\hat{R}}{\displaystyle\int_{R_{min}(E_0,p_{g0},We)}^{R_{max}(E_0,p_{g0},We)} \frac{\sqrt{\hat{R}^3}\mathrm{d}\hat{R}}{\sqrt{2\left\{E_0 + p_{g0}\ln(\hat{R}) - \frac{\hat{R}^2}{We} - \frac{\hat{R}^3}{3}\right\}}}},$$

where the right-hand side is expressed entirely as a function of the Reynolds number $Re = \rho U \bar{R}_M/\mu$, $E_0$, the dimensionless minimum pressure $p_{g0}$ at the maximum bubble radius during the first cycle, the Weber number $We = \bar{R}_M\Delta/\sigma$ in which $U = \sqrt{\Delta/\rho}$, $\rho$ and $\mu$ are the density and viscosity of the liquid surrounding the bubble, respectively. Furthermore, $R_{max}(E_0, p_{g0}, We)$ and $R_{min}(E_0, p_{g0}, We)$ are the maximum and minimum radii of the bubble, respectively. The initial condition for the energy of a bubble system is given by

$$E_0(0) = \frac{1}{We} + \frac{1}{3}.$$

Secondly, the maximum radius $R_{max}(E_0, p_{g0}, We)$ and the minimum radius $R_{min}(E_0, p_{g0}, We)$ are given as the two successive roots of

$$E_0 + p_{g0}\ln(R_0) - \frac{R_0^2}{We} - \frac{R_0^3}{3} = 0.$$

Thirdly, we express the frequency $\omega$ in terms of $E_0$, $p_{g0}$ and $We$ via

$$\omega(E_0, p_{g0}, We) = \frac{\pi}{\displaystyle\int_{R_{min}(E_0,p_{g0},We)}^{R_{max}(E_0,p_{g0},We)} \frac{\sqrt{\hat{R}^3}\mathrm{d}\hat{R}}{\sqrt{2\left\{E_0 + p_{g0}\ln(\hat{R}) - \frac{\hat{R}^2}{We} - \frac{\hat{R}^3}{3}\right\}}}}.$$

These equations allow the calculation of the energy $E_0(t_v)$, the frequency $\omega$, the maximum radius $R_{max}$ and the minimum radius $R_{min}$ without prior knowledge of the leading-order solution $R_0$.

## REFERENCES


[1]F. R. Young, *Cavitation* (McGraw-Hill, 1989).

[2]T. G. Leighton, *The Acoustic Bubble* (Academic Press, London, 1994).

[3]A. Prosperetti, "Bubbles," Phys. Fluids **16**, 1852–1865 (2004).

[4]C. E. Brennen, *Cavitation and Bubble Dynamics* (Cambridge University Press, 2013).

[5]L. Rayleigh, "On the pressure developed in a liquid during the collapse of a spherical cavity," Phil. Mag. **34**, 94–98 (1917).

[6]M. S. Plesset, "The dynamics of cavitation bubbles," ASME J. Appl. Mech. **16**, 277–282 (1949).

[7]B. E. Noltingk and E. A. Neppiras, "Cavitation produced by ultrasonics," Proc. Phys. Soc. Lond. **63B**, 674–685 (1950).

[8]E. A. Neppiras and B. E. Noltingk, "Cavitation produced by ultrasonics: theoretical conditions for the onset of cavitation," Proc. Phys. Soc. Lond. **64B**, 1032–1038 (1951).

[9]H. Poritsky, "The collapse or growth of a spherical bubble or cavity in a viscous fluid," in *Proc. First Nat. Cong. in Appl. Math.* (1952) pp. 813–821.

[10]W. Lauterborn and T. Kurz, "Physics of bubble oscillations," Rep. Prog. Phys. **73**, 106501 (2010).

[11]D. Obreschkow, M. Bruderer, and M. Farhat, "Analytical approximation for the collapse of an empty spherical bubble," Phys. Rev. E **85**, 066303 (2012).

[12]P. Amore and F. M. Fernández, "Mathematical analysis of recent analytical approximations to the collapse of an empty spherical bubble," J. Chem. Phys. **138**, 084511 (2013).

[13]N. A. Kudryashov and D. I. Sinelshchikov, "Analytical solutions of the Rayleigh equation for empty and gas-filled bubble," J. Phys. A: Math. Theor. **47**, 405202 (2014).

[14]S. C. Mancas and H. C. Rosu, "Evolution of spherical cavitation bubbles: Parametric and closed-form solutions," Phys. Fluids **28**, 022009 (2016).

[15]A. R. Klotz, "Bubble dynamics in N dimensions," Phys. Fluids **25**, 082109 (2013).

[16]N. A. Kudryashov and D. I. Sinelshchikov, "Analytical solutions for problems of bubble dynamics," Phys. Lett. A **379**, 798–802 (2015).

[17]R. A. Van Gorder, "Dynamics of the Rayleigh-Plesset equation modelling a gas-filled bubble immersed in an incompressible fluid," J. Fluid Mech. **807**, 478–508 (2016).

[18]S. G. Zhang, J. H. Duncan, , and G. L. Chahine, "The final stage of the collapse of a cavitation bubble near a rigid wall," J. Fluid Mech. **257**, 147–181 (1993).

[19]S. G. Zhang and J. H. Duncan, "On the nonspherical collapse and rebound of a cavitation bubble," Phys. Fluids **6**, 2352–2362 (1994).

[20]A. Philipp and W. Lauterborn, "Cavitation erosion by single laser-produced bubbles," J. Fluid Mech. **361**, 75–116 (1998).

[21]Q. X. Wang, "Multi-oscillations of a bubble in a compressible liquid near a rigid boundary," J. Fluid Mech. **745**, 509–536 (2014).

[22]E. Klaseboer, S. W. Fong, C. K. Turangan, B. C. Khoo, A. J. Szeri, M. L. Calvisi, G. N. Sankin, and P. Zhong, "Interaction of lithotripter shockwaves with single inertial cavitation bubbles," J. Fluid Mech. **593**, 33–56 (2007).

[23]Q. X. Wang and J. R. Blake, "Non-spherical bubble dynamics in a compressible liquid. Part 1. Travelling acoustic wave," J. Fluid Mech. **659**, 191–224 (2010).

[24]Q. X. Wang and J. R. Blake, "Non-spherical bubble dynamics in a compressible liquid. Part 2. Acoustic standing wave," J. Fluid Mech. **679**, 559–581 (2011).

[25]Q. X. Wang and K. Manmi, "Microbubble dynamics near a wall subjected to a travelling acoustic wave," Phys. Fluids **26**, 032104 (2014).

[26]Q. X. Wang, K. Manmi, and K. Liu, "Cell mechanics in biomedical cavitation," Interface Focus **5**, 20150018 (2015).

[27]K. S. Suslick and L. A. Crum, "Sonochemistry and sonoluminescence," in *Encyclopedia of Acoustics*, edited by M. J. Crocker (Wiley-Interscience, New York, 1997) pp. 271–282.

[28]C. D. Ohl, M. Arora, R. Ikink, N. de Jong, M. Versluis, M. Delius, and D. Lohse, "Sonoporation from jetting cavitation bubbles," Biophys. J. **91**, 4285–4295 (2006).

[29]G. E. Kuzmak, "Asymptotic solutions of nonlinear second order differential equations with variable coefficients," Prikl. Mat. Mekh. **23**, 515–526 (1959), (In Russian) J. Appl. Math. Mech., 23 (1959), pp. 730-744.(In English).

[30]J. C. Luke, "A perturbation method for nonlinear dispersive wave problems," Proc. Roy. Soc. Lond. A **292**, 403–412 (1966).

[31]W. R. Smith, "Modulation equations for strongly nonlinear oscillations of an incompressible viscous drop," J. Fluid Mech. **654**, 141–159 (2010).

[32]W. R. Smith and J. G. Wissink, "Travelling waves in two-dimensional plane Poiseuille flow," SIAM J. Appl. Math. **75**, 2147–2169 (2015).

[33]Z. C. Feng and L. G. Leal, "Nonlinear bubble dynamics," Annu. Rev. Fluid Mech. **29**, 201–243 (1997).

[34]A. Prosperetti, "A generalization of the rayleigh-plesset equation of bubble dynamics," Phys. Fluids **25**, 409–410 (1982).

[35]L. Bergamasco and D. Fuster, "Oscillation regimes of gas/vapor bubbles," Int. J. Heat Mass Transfer **112**, 72–80 (2017).

[36]J. B. Keller and I. I. Kolodner, "Damping of underwater explosion bubble oscillations," J. Appl. Phys. **27**, 1152–1161 (1956).

[37]J. B. Keller and M. Miksis, "Bubble oscillations of large amplitude," J. Acoust. Soc. Am. **68**, 628–633 (1980).

[38]A. M. Shapiro and M. I. Weinstein, "Radiative decay of bubble oscillations in a compressible fluid," SIAM J. Math. Anal. **43**, 828–876 (2011).

[39]O. Costin, S. Tanveer, and M. I. Weinstein, "The lifetime of shape oscillations of a bubble in an unbounded, inviscid, and compressible fluid with surface tension," SIAM J. Math. Anal. **45**, 2924–2936 (2013).

[40]A. Prosperetti and A. Lezzi, "Bubble dynamics in a compressible liquid. Part. 1. First-order theory." J. Fluid Mech. **168**, 457–478 (1986).

[41]A. Lezzi and A. Prosperetti, "Bubble dynamics in a compressible liquid. Part. 2. Second-order theory." J. Fluid Mech. **185**, 289–321 (1987).

[42]Q. X. Wang, "Non-spherical bubble dynamics of underwater explosions in a compressible fluid," Phys. Fluids **25**, 072104 (2013).

[43]Q. X. Wang, "Local energy of a bubble system and its loss due to acoustic radiation," J. Fluid Mech. **797**, 201–230 (2016).

[44]J. Kevorkian and J. D. Cole, *Perturbation methods in applied mathematics* (Springer, New York, 1981).

[45]W. R. Smith, "On the sensitivity of strongly nonlinear autonomous oscillators and oscillatory waves to small perturbations," IMA J. Appl. Math. **70**, 359–385 (2005).

[46]W. R. Smith, J. R. King, B. Tuck, and J. W. Orton, "The single-mode rate equations for semiconductor lasers with thermal effects," IMA J. Appl. Math. **63**, 1–36 (1999).

[47]A. Wolf, C. Rauh, and A. Delgado, "Dynamics and long-time behavior of a small bubble in viscous liquids with applications to food rheology," Arch. Appl. Mech. **86**, 979–1002 (2016).

[48]M. S. Plesset and A. Prosperetti, "Bubble dynamics and cavitation," Ann. Rev. Fluid Mech. **9**, 145–185 (1977).

[49]H. Lamb, *Hydrodynamics*, sixth ed. (Cambridge University Press, 1932).

[50]P. H. Roberts and C. C. Wu, "The decay of bubble oscillations," Phys. Fluids **10**, 3227–3229 (1998).